Assessment of the recurrence intervals of rockfall through dendrogeomorphology and counting scar approach: A comparative study in a mixed forest stand from the Vercors massif (French Alps)

Robin Mainieri, Jérôme Lopez-Saez, Christophe Corona, Markus Stoffel, Franck Bourrier, Nicolas Eckert

Assessment of the recurrence intervals of rockfall through dendrogeomorphology and counting scar approach: a comparative study in a mixed forest stand from the Vercors massif (French Alps).

Robin Mainieri[1, 2], Jérôme Lopez-Saez[3], Christophe Corona[4], Markus Stoffel[3,5,6], Franck Bourrier[1], Nicolas Eckert[2]

1 Univ. Grenoble Alpes, Irstea, UR LESSEM, 2 rue de la Papeterie-BP 76, F-38402 St-Martin-d'Hères, France

2 Univ. Grenoble Alpes, Irstea, UR ETGR, 2 rue de la Papeterie-BP 76, F-38402 St-Martin-d'Hères, France

3 Institut des Sciences de l'Environnement – Université de Genève, 66 bd Carl Vogt, CH-1205 Genève, Suisse

4 GEOLAB, UMR6042 CNRS / Université Blaise Pascal, Maison des sciences de l'homme, 63057 Clermont-Ferrand Cedex 2, France

5 Dendrolab.ch, Department of Earth Sciences, University of Geneva, 13 rue des Maraîchers, CH-1205 Geneva, Switzerland

6 Department F.A. Forel for Environmental and Aquatic Sciences, University of Geneva, 66 Boulevard Carl-Vogt, CH-1205 Geneva, Switzerland

Keywords *: Rockfalls, Recurrence interval, Tree-ring analyses, French Alps*

Abstract

As direct observations of rockfalls are rare and difficult to obtain over long timescales, stem injuries and their dating with dendrogeomorphic techniques have been applied frequently in the past to reconstruct process activity. However, the analysis of tree-ring samples requires considerable temporal efforts, which can be detrimental in applied research and expert opinions. To compensate for this shortcoming, several studies have lately explored the potential of the counting of visible scars as an alternative method to dendrogeomorphology as it requires much less time and human efforts to reconstruct spatial patterns of rockfall activity. Yet, to date, both approaches have not been compared at the same site. In this paper, based on the extensive analysis of 278 conifer and broadleaved trees (from which 1097 tree-ring cores were extracted) from a mixed forest plot of the Vercors Massif (French Alps), we demonstrate that both methods provide similar spatial patterns of rockfall activity with a strong increase of recurrence intervals down the talus slope and a clear lateral zonation of activity. Despite this apparent convergence between both approaches, our study also evidences that rockfall frequencies strongly differ with tree species and diameter: the visual inspection of conifer stems and the analysis

of tree-ring signals in large-diameter broadleaved trees typically lead to an overestimation of recurrence intervals. Based on these findings, we recommend giving priority to the scar-counting approach on small diameter (<15cm) broadleaved stems and to restrict tree-ring analysis to old conifers that are more susceptible – through the identification of tangential rows of traumatic resin ducts – to provide reliable estimations of long recurrence intervals (as generally observed in the lower portions of the slope). These guidelines should help to improve the reliability of recurrence interval maps of rockfall process activity in forests further, but also to improve cost-benefit ratios of future studies.

1. Introduction

Rockfalls are widespread natural hazards in mountain regions where they threaten inhabited areas and transport corridors, causing each year significant economic and human losses (Volkwein et al., 2011). They are commonly defined as the detachment of a rock fragment from a steep rock wall (Selby, 1993) which then travels some distance down the slope by bouncing, falling or rolling (Varnes, 1978). In general, fragmental rockfalls involve relatively small detachments of isolated rocks or/and boulders with maximum volumes normally remaining <30 m^3 (Dorren et al., 2007). Despite their limited volumes, rockfalls pose a significant hazard, due to their rapid evolution, high velocity and impact energy, but their unpredictable occurrence hinders detailed investigation of their dynamics and drivers under natural conditions. Typical approaches to deliver information about rockfalls include (i) deterministic and probabilistic susceptibility analysis (Dietze et al., 2017), (ii) predictive modelling of their potential propagation (Dorren et al., 2003), (iii) *a posteriori* mapping of detachment zones, released volumes and trajectories by aerial and satellite imagery, repeat terrestrial laser scan (TLS), rockfall collector surveying (Sass et al., 2005; Abellán et al., 2010) or seismic cliff monitoring (Dietze et al., 2017) as well as (iv) rockfall inventories (Hungr et al., 1999; Dussauge, 2003). However, major efforts are still required to quantify rockfall activity in terms of frequency and magnitude at the local scale, which is crucial for risk assessment, the choice of appropriate mitigation measures, and for the validation of output from simulation runs.

On forested slopes, trees are reliable bio-indicators of past rockfall activity (Stoffel and Corona, 2014). Dendrogeomorphology – an approach based on the analysis of damage inflicted to trees after rockfall impacts – can be used to overcome certain gaps and limitations inherent to historical archives (Ibsen and Brunsden, 1995; Sass and Oberlechner, 2012). Indeed, tree-ring reconstructions have been used in the past to (i) compute the

frequency of past events (Stoffel, 2006; Trappmann et al., 2014), (ii) map preferential trajectories of rockfalls, (iii) identify climatic drivers of rockfall activity (Schneuwly and Stoffel, 2008a; Šilhán et al., 2011) as well as to (iv) compare observed and/or reconstructed rockfall inventories with process activity as predicted by three-dimensional, process-based rockfall models (Stoffel et al., 2006; Corona et al., 2013; Corona et al., 2017. Table 1 provides a synthesis of rockfall research realized with tree rings). The main weakness of these dendrogeomorphic approaches is the substantial time effort required for exhaustive sampling (with cross-sections and cores), identification, cross-dating, and dating of growth disturbances forming after mechanical disturbance by rockfall impacts. Trappmann and Stoffel (2013, 2015) and Favillier et al. (2017) have suggested the counting of visible scars as an alternative method requiring much less time and efforts as compared to conventional dendrogeomorphic approaches when it comes to the reconstruction of spatial patterns of rockfall activity. Yet, to date, the two approaches have not been compared systematically at a single site and for a common dataset.

In this context, based on a procedure that includes (i) an extraction of a representative number of trees from an exhaustive forest inventory, (ii) the estimation of tree ages from allometric curves and increment cores as well as (iii) the quantification of rockfall-related growth disturbances based on the visual inspection of stems and tree-ring analyses, this paper aims at comparing recurrence interval maps derived from both approaches so as to evaluate their respective reliability as well as their advantages and inconveniences. To quantify potential biases related to tree species in rockfall frequency estimation, as previously evidenced by Trappmann and Stoffel (2013) and Favillier et al. (2017), our study was conducted in a mid-altitude (1500 m asl) mixed forest stand from the Vercors massif (French Alps).

2. Study site

The study site is located in the municipality of Saint-Guillaume (256 inhabitants) on the northern slope of the Pale mountain, at a locality named “Rocher du Bouchet” (44°56'18"N, 5°35'11"E, 1350 - 1490 m asl, Fig. 1a). At this site, rockfall is frequent and fragments are normally detached from several release zones of a roughly 90-m-high north-east-facing cliff (1450-1540 m asl, Fig. 1b). Bedrock in the release areas is composed of subhorizontally bedded Jurassic limestone (Tithonian) with narrow orthogonal joints which favor the release of small rock fragments with volumes ranging from a few dm^3 to a few m^3 (Fig. 1e). In the adjacent transit area

(1380–1490 m asl) Quaternary deposits are mainly composed of a scree talus covered by a mixed forest stand. This scree slope is characterized by a marked longitudinal sorting of debris with volumes of a few dm^3 at the apex to a few m^3 in the lower portion. The angle of the talus slope varies between 26° and 46° (average: 38°). The bottom of the slope, located at an altitude of ~ 1100 m, is limited by a topographic berm (10°).

The tree plot area analyzed here (Fig. 1c) is located at the foot of the cliff. The plot is about 1 ha (110 × 90 m) in size and is covered by a dense (800 trees ha^{-1}) mixed forest stand mainly composed of *Abies alba* (Silver fir), *Picea abies* (Norway spruce), *Acer pseudoplatanus* (Sycamore maple), *Fagus sylvatica* (Common beech), *Fraxinus excelsior* (European ash), *Sorbus aria* (White beam), *Sorbus aucuparia* (Mountain ash) and *Ulmus glabra* (Elm). Evidence of past logging (stumps) is lacking at the study site, yet some silvicutural exploitation over the course of the last century cannot be ruled out completely. Average annual rainfall (1961-2013) at the Grenoble meteorological station (45°09'58"N, 5°45'58"E, 220 m asl), located 40 km North of the study site, is 934 mm. Average mean air temperature is 12.5 ° C. Rockfall is the dominant geomorphic process on the slope and is responsible for a vast majority of the scars observed on the tree stems. Other geomorphic processes cannot be totally excluded, especially in the uppermost portions of the talus slope, where snow avalanches of limited extent are susceptible to occur. No data on past geomorphic events exist in municipal records.

3. Material and methods

3.1. Preliminary step: systematic tree plot

In a first step, a full tree positioning and mapping procedure was used so as to build a database for the assessment of rockfall activity at the site. Trees with a diameter at breast height (DBH) > 5 cm were systematically located in the 110 × 120 m tree plot orientated perpendicular to the line of maximum slope gradient (Fig. 1c, 2a). The position of each tree was determined with decimetric precision using a sonic rangefinder, compass, and inclinometer. Information on tree species and diameter was recorded in a database. In total, 793 trees were positioned in a geographical information system (GIS) as geo-objects. This systematic tree plot was then used as a basis for a stratified random sampling strategy. To this end, the initial tree population was divided into five sub-groups (DBH<15 cm, 15-25cm, 25-40cm, 40-60cm, >60cm), on the basis of tree species and diameter. The size of each subgroup, fixed so as to be representative of the diameter spectrum observed at the stand scale, thereby varied between n=19 for DBH>60cm and n=39 for DBH=15-25cm. Each

randomly selected stem was visually inspected and cored with an increment borer with the final aim of comparing the scar counting and the dendrogeomorphic approaches.

3.2. The visual scar-counting approach

Trappmann and Stoffel (2013, 2015) and Favillier et al. (2017) have previously demonstrated the reliability of the visual scar-counting approach to reconstruct spatial patterns of rockfall activity. For each tree extracted from the random sampling, recent scars were thus identified according to their appearance, chipped bark, or injured wood, following the approach described by Trappmann and Stoffel (2015). Wounds that were about to overgrow at the time of sampling were identified by the callus pad sealing the injuries from the margin toward the center (Stoffel and Perret, 2006, Fig. 1d). Older, completely healed injuries were more difficult to be detected visually, especially in tree species with thick barks (Stoffel and Perret, 2006); they were inferred via the occurrence of "swellings" and blisters on the stem surface. Extremely long, vertical scars or scars with vertical extensions < 3 cm were excluded to avoid misclassification and/or the inclusion of injuries caused by branch breakage or falling neighboring trees (Perret et al., 2006).

3.3. Development of age–diameter regression models

In a second step, logarithmic diameter-age regression models (Rozas, 2003) were built for the conifer (P. abies, A. alba) and broadleaved (*A. pseudoplatanus, F. sylvatica, F. excelsior, S. aria, S. aucuparia, U. glabra*) tree species at the stand scale. To this end, a total of 109 undisturbed trees with a DBH ≥ 10 cm were cored using a Pressler increment borer. Trees were selected according to five diameter classes, representative at the tree plot scale. Samples were analyzed and data processed following standard dendrochronological procedures (Bräker, 2002). In the laboratory, tree rings were counted using a digital LINTAB positioning table connected to a Leica stereomicroscope. Missing rings toward the pith were estimated from ring curvature (Villalba and Veblen, 1997; Bollschweiler et al., 2008). In a final step, we used data from the logarithmic regression models to estimate tree ages of individual trees selected from random sampling for which scars were identified and counted on the stem surface and for which the DBH has been measured.

3.4. Dendrogeomorphic analyses

As our study aims at comparing the recurrence intervals of rockfalls derived from the scar-counting approach and from classical dendrogeomorphic analysis, event histories at the level of individual trees were reconstructed as well through the analysis of tree-ring sequences. For each tree extracted from the random sampling, an increment core (max. 40×0.5 cm) was taken at the lateral edges of each visible scar (i.e. at the contact of the unaffected wood with the overgrowing callus tissue; Sachs 1991, Larson 1994; Schneuwly and Stoffel, 2008b). For this investigation, the first layer of callus tissue within the tree-ring was used to determine the timing of rockfall activity. For conifers, known to mask injuries efficiently, tangential rows of traumatic resin ducts (TRDs; Bannan, 1936; Stoffel and Bollschweiler, 2008) formed next to and at some distance of the impact scar (Schneuwly et al., 2009a, 2009b) were used as a further indicator to date past rockfalls (Stoffel, 2006). Resin ducts were only considered the result of rockfall activity if they formed traumatic, compact, continuous and tangential rows (Stoffel et al., 2005a). In addition, based on the distribution of observed scars (which remain usually below 2m at the study site), one increment core was systematically extracted, in the fall line, at 0.5, 1.0, and 1.5 m, in order to increase the likelihood to retrieve old, completely healed impacts. The 0.5 m core was also used to estimate the cambial age of each tree.

Following Stoffel et al. (2005 a, b), (i) abrupt suppression of tree growth indicating decapitation or branch loss, (ii) presence of callus tissue and TRD next to (blurred) injuries; (iii) eccentric growth and the formation of reaction wood following stem tilting; and (iv) abrupt growth release (suggesting that neighboring trees were eliminated and the surviving trees benefited from improved growth conditions such as enhanced access to light, water, and nutrients) were used as additional evidence of past rockfall impacts.

3.5. Estimation of recurrence interval of individual rockfall impacts

The assessment of recurrence interval is a classical concept that is regularly used in the analysis of all types of hazards, but it was only introduced very lately into dendrogeomorphology to inform avalanche zoning (Corona et al., 2010; Schläppy et al., 2013; Favillier et al., 2018) or rockfall risk assessments (Šilhán et al., 2013; Trappmann et al., 2014, Favillier et al., 2015, 2017). In dendrogeomorphology, recurrence intervals represent the average time passing between two successive impacts at a specific point (i.e., the surface of an individual tree for which the position on the slope is known) as follows:

$$RiV = \frac{AVt}{ScVt} \quad (1)$$

$$RiD = \frac{ADt}{ScD} \quad (2)$$

where *RiV* and *RiD* represent the recurrence intervals computed from the visual scar-counting and dendrogeomorphic approaches, respectively; AV_t and AD_t indicate the age of each tree as derived from the dendrometric assessment and tree-ring countaing, respectively; and ScV_t and ScD_t show the number of scars that were visually observed on each stem t and retrieved from tree-ring analysis, respectively.

The study area was clustered into ~55 m × 30 m cells for further analysis (Fig. 1c). Mapped trees were then assigned to cells according to their location. The distributions of tree ages, growth disturbances, and recurrence intervals were compared at the plot and cell scales. A systematic comparison was also realized between conifer and broadleaved trees. Due to their non-normal distributions, the non-parametric Wilcoxon-Mann-Whitney (WMW) test was used to compare tree ages, growth disturbances, and recurrence intervals for conifer and broadleaved trees at the plot and cell scales.

4. Results

4.1. Recurrence intervals derived from the scar-counting approach

The logarithmic diameter-age regression models for the conifer and broadleaved tree species at the tree plot are given by the following equations:

$$Age\_B_t = 50.148ln(D_t) - 57.696 \quad (n = 43, r^2 = 0.61, p < 0.001) \quad (3)$$

$$Age\_C_t = 49.545\ ln(D_t) - 62.907 \quad (n = 66, r^2 = 0.67, p < 0.001) \quad (4)$$

where Age_B_t and Age_C_t represent the estimated ages for each broadleaved and conifer tree (t), respectively; and where $ln(D_t)$ represents the Neperian logarithm diameter of tree t.

According to these models, conifers grow faster than broadleaved trees. Conifer and broadleaved trees with radii of 20 cm are theoretically aged 93 and 85 years, respectively. The oldest conifer (*A. alba*) randomly extracted from the tree plot was 236 years old (DBH = 112 cm) whereas the oldest broadleaved tree (*F. sylvatica*) was only 176 years old (DBH = 176 cm). At our study plot, and according to the diameter-age regression models, the 278 trees randomly extracted from the tree plot averaged 90 ± 35 years (i.e. 87 ± 30 years for 99 broadleaved trees and 91 ± 37 years for 179 conifers). The Wilcoxon-Mann-Whitney test revealed that the distributions by tree species are not statistically different.

187 On the basis of the scar-counting approach, 815 scars (475 on conifers, 340 on broadleaved trees) were
188 identified on the 278 stems that were randomly extracted and visually inspected. A total of 39 of the selected
189 trees (14%) did not present any visual evidence of past rockfall impacts. On average, 2.9 (± 2.4) injuries were
190 counted on tree stems, 3.4 (± 2.5) and 2.6 (± 2.3) on broadleaved and conifer trees, respectively. Noteworthy,
191 both distributions are statistically different ($p < 0.05$). From a spatial perspective, the scar-counting approach
192 clearly evidences the existence of a downslope gradient in scar numbers. The average number of injuries per
193 stem thus decreases from 4.4 on the top third of the plot (cell B) to 3.2 in the central part (cell D), and 1.9 on the
194 lower third (cell F). Cell E (0.9 scar.stem^{-1}) appears as the least active area within our study plot.
195 At the plot scale, recurrence intervals of rockfall were computed as the ratio between tree ages estimated from
196 regression models and the number of injuries observed on each tree stem. Based on the data used, the average
197 recurrence interval is 38 years. The distributions of *RiV* statistically differ ($p < 0.05$) between conifer (mean: 45
198 years) and broadleaved (mean: 31 years) trees. The recurrence interval map (Fig. 3a) exhibits an increasing trend
199 as one moves down the slope: the average time elapsed between two consecutive scars by the scar-counting
200 approach gradually increases from an average of 15-25 years in the top third of the slope (cells A–B) to reach
201 values of 50-150 years in the lowest third of the plot (cells E–F), at the level of the topographic berm. The map
202 also evidences a clear lateral zonation pattern with more frequent rockfalls observed in the northwestern part of
203 the plot (*RiV* = 25 and 51 years in cells B and D, respectively) as compared to its eastern counterpart (*RiV* = 52
204 and 67 years in cells A and C, respectively). Except for cell B ($p < 0.05$), recurrence intervals estimated from
205 broadleaved and conifers trees were not statistically different (Fig.4).

206 *4.2. Recurrence intervals derived from tree-ring analysis*

207 In total, 1097 increment cores have been sampled on the 278 impacted stems. On average, tree ages were
208 comparable for conifer (85 ± 42 years) and for broadleaved trees (84 ± 44 years) and their distributions did not
209 differ statistically. In total, dendrochronological analysis allowed identification of 810 rockfall events (207 on
210 broadleaved trees and 603 on conifers), mainly detected in the form of injuries (55%), tangential rows of
211 traumatic resin ducts (TRDs, 24%), and growth suppressions (16%) (Tab. 2). The mean number of growth
212 disturbances (GDs) per stem (2.9 ± 2.7 GD) was greater for conifers (3.4± 2.8 GD) than for broadleaved trees (2.1
213 ± 2 GD). Amongst the 810 reconstructed events, 243 (30%) were reconstructed from growth disturbances that
214 were not visible on the stem surface, mainly in the form of overgrown injuries (38%), TRDs (31%) and growth

suppressions (26%). The percentage of growth disturbances retrieved from increment cores but not visible on the stem surface was significantly higher on conifers than on broadleaved trees (36 and 10%, respectively). The ratio between visible and invisible growth disturbances (GD) exceeded 45% for conifers > 25 cm, but was only 10% for large-diameter broadleaved trees (Fig. 5).

At the plot scale, the recurrence interval is 32 years on average and the distributions of *RiD* statistically differ ($p<0.05$) between conifer (mean: 30 years) and broadleaved (46 years) trees. In spatial terms, the *RiD* increases from 10-25 years in the upper third of the study plot to 50-150 years in its lower part. A lateral gradient is superimposed on this longitudinal zonation: more frequent activity is thus observed in cells B, D, and F (*RiD* = 21, 45, and 65 years, respectively) than in cells A, C, and E (*RiD* = 49, 63, and 90 years, respectively) (Fig. 3b). According to the Wilcoxon-Mann-Whitney test, distributions of recurrence intervals from broadleaved and conifer trees are statistically different in cells D and E ($p < 0.05$) (Fig. 6).

4.3. Comparison of both approaches

To compare both approaches, we computed differences between tree ages, number of GDs and recurrence intervals between the scar-counting and dendrogeomorphic analyses and at the scale of individual trees. With respect to tree ages estimated from the (i) age-diameter relation and (ii) the dendrogeomorphic approach, the mean difference between both approaches was 7 years. Noteworthy, however, the difference was in the range ±20 years in 50% of the trees (46% for conifers, 54% for broadleaved trees), and exceeded 50 years in 35 trees (12.5%; 17 conifers and 18 broadleaved trees). Differences clearly increased with stem diameter (Figs. 3c, 3d,7a), yet, age distributions derived from logarithmic regressions and tree-ring analyses were not statistically different.

In 25% of the trees (n=69), the number of injuries counted at the stem surface was equal to the number of growth disturbances in the tree-ring series. The differences ranged between -2 and +2 scars for 78.5% of the trees, and exceeded 5 scars on 15 trees (5%). In the case of the conifers, the number of growth disturbances retrieved from tree-ring analysis was frequently greater than the number of injuries observed on the stem surface (Fig. 7b). Conversely, in the case of broadleaved trees, the visual counting approach tended to overestimate the number of injuries. According to Fig. 7b, these differences were not diameter-dependent. From a spatial perspective, the number of scars observed on broadleaved stems exceeded the number of GDs

detected in the tree-ring series significantly ($p < 0.05$) in cells B, D, and E. In the case of conifers, differences between both approaches were significant in the lower third of the plot in cells E and F.

In 42.5% (n = 119) of all trees, differences between the scar counting and the dendrogeomorphic analyses were less than 10 years in terms of recurrence intervals. In 14% of the stems, values, however, exceeded 50 years. According to the Wilcoxon-Mann-Whitney test, *RiV* and *RiD* distributions (fig. 7c) did not differ statistically, neither at the plot nor at the cell scales. Paradoxically, differences between the mean recurrence interval computed from the visual and dendrogeomorphic series were statistically significant at the 5% level if conifer and broadleaved trees were considered separately at the plot scale. Unsurprisingly, the recurrence interval maps showed comparable downslope gradients and confirmed the difference between the northwestern and southeastern compartments of the plot analyzed in this study. At the cell scale, recurrence intervals derived from both approaches differed ($p < 0.05$) for broadleaved trees in the northwestern (cells B and D) and for conifers in the lower (cells E and F) compartments of the plot.

5. Discussion

5.1. Convergence between the scar-counting and the dendrogeomorphic approaches

Long-term records of rapid mass movements, such as rockfalls, have proven to be limited. This lack of inventories is especially detrimental in urbanized areas (Dorren et al., 2007; Volkwein et al., 2011) where risk is often increasing disproportionally with ongoing urbanization (Baillifard et al., 2004). In these areas, finding ways that allow precise reconstruction of past rockfall activity are urgently needed. In case that such slopes are forested, growth disturbances in trees are a reliable option that allows one to reconstruct past rockfall activity in the absence of any inventory or clear morphological evidence, such as scree slopes or isolated blocks (Volkwein et al., 2011) by , either inspecting stems visually (Trappmann and Stoffel, 2013; Favillier et al., 2015, 2017; Eichenberger et al., 2017) or by analyzing the tree-ring records of impacted trees (Alestalo, 1971; Stoffel et al., 2010). Based on a stratified, random sampling of 278 trees from an exhaustive mapping of 1004 trees in a mixed forest stand, we compared, for the first time, recurrence intervals derived from both approaches in a 1-ha plot. The systematic counting of visible scars yielded 810 records on all tree stems and the dendrogeomorphic approach allowed identification of 815 growth disturbances in tree-ring series.

268 This comparison represents a significant improvement with respect to former studies. Indeed, whereas Favillier
269 et al. (2015) showed that significant differences exist in recurrence intervals between *Acer opalus* and *Quercus*
270 *pubescens* based on scar counting, they did not compare their result with tree-ring analyses. Trappmann and
271 Stoffel (2013) compared both approaches but used tree-ring analysis from a conifer species (*Picea abies*) and
272 visual scar counting on broadleaved trees (*F. sylvatica*). They concluded that the absolute numbers of rockfalls
273 (and hence return intervals) vary significantly between the approaches, and that the mean number of rockfalls
274 observed on the stem surface of *F. sylvatica* exceeds that of *P. abies* by a factor of ~3. On the other hand, both
275 methods yielded comparable data on the spatial distribution of relative rockfall activity.
276 Based on the results of this study, Fig 8 synthesizes the recurrence intervals obtained from both approaches, at
277 the plot (Fig. 8a) and cell (Fig. 8 b-g) scales, and for conifer and broadleaved species. At the plot scale, mean
278 recurrence intervals (38 and 32 years) computed from both approaches are comparable. The marked downslope
279 decrease in the number of observed scars per stem is consistent with the well-known frequency reduction of
280 fallen blocks down the slope (Gsteiger, 1989; Dorren et al., 2005, 2006, 2007). In addition, both approaches
281 converge to show a clear difference between the northwestern (more active) and eastern (less active)
282 compartments of the plot. This convergence is confirmed regardless of the cell considered, and the Wilcoxon-
283 Mann-Whitney test does not point to any significant difference in mean recurrence intervals between the scar-
284 counting and dendrogeomorphic methods. These results suggest that the visual scar counting (Trappmann and
285 Stoffel, 2013; Favillier et al., 2017) represents an efficient and effective alternative to the time-consuming
286 dendrogeomorphic approach when it comes to the spatial assessment of rockfall activity on larger surfaces, as it
287 can be realized with limited temporal and financial efforts.

288 *5.2. Differences between conifers and broadleaved trees*

289 Despite the overall convergence of both approaches based on the full dataset of trees, one should keep in mind
290 that rockfall recurrence intervals differ strongly as soon as conifer or broadleaved trees are considered
291 separately. At the plot scale, these differences in return periods computed from both approaches amount to +14
292 years and -16 years for broadleaved and conifer trees, respectively (Fig. 8). In other words, the number of
293 injuries counted on conifer stems is lower than the number of growth disturbances retrieved from the
294 dendrogeomorphic approach. By contrast, in the case of broadleaved trees, the visual inspection tends to
295 overestimate the frequency of past rockfall activity. The fact that comparable mean recurrence intervals are

obtained from the full dataset therefore results from a compensatory effect, meaning that higher recurrence intervals computed from the visual inspection of broadleaved trees are counterbalanced by lower intervals derived from conifer trees. Similarly, the more frequent growth disturbances identified in the tree-ring series of conifers compensate for the reduced number of injuries retrieved from the tree-ring series of broadleaved trees. The main reason for such interspecific differences are the hidden scars. The masking of wounds can be highly variable as a result of the initial size of the injury, vitality of the tree, its genetic capability to overgrow injuries, bark structure, annual increment rates, or tree age, just to name a few reasons. Yet, in general, tree species with a thick and structured bark will mask scars more efficiently than those with thin and smooth bark structures (Stoffel and Perret, 2006; Trappman and Stoffel, 2013; Favillier et al., 2015). Stoffel (2005), for instance, could identify 75% of all scars by visual interpretation of bark structures on *F. sylvatica*, whereas only 51% of the injuries remained visible on the stem surface of *P. abies*.

At our study site, we can reliably assume that thick-barked conifer trees mask scars of past events very efficiently. As a consequence, old scars are difficult to detect, unless wound callus pads remain clearly visible on the stem surface (Larson, 1994; Fink, 1999). One could argue that the rapid healing could also render the determination of suitable coring positions a difficult task and that older events could be missed on increment cores as well. Yet, the dominant conifer species, *A. alba*, *P. abies*, both react to mechanical damage with the formation of tangential rows of traumatic resin ducts (Lepage and Bégin 1996; Stoffel and Perret 2006; Bollschweiler et al. 2008) with a tangential spread on more than one-third of the circumference (Schneuwly and Stoffel, 2008b). These TRDs that represent one-fourth of the GD dated in the tree-ring series therefore make it possible to overcome the difficulty related to masked scars.

By contrast, broadleaved species generally have a thinner and smoother bark structure which not only facilitates wounding but also enhances longer-term visibility of scars on the stem surface (Stoffel, 2005; Stoffel and Perret, 2006). Based on micro-section analyses, Arbellay et al. (2010, 2012) demonstrated that injured rings of *Betula pendula* and *Fraxinus excelsior* were characterized by smaller vessels. Yet, these anatomical changes were only visible in a 30° radial segment around the injury. Arbellay et al. (2012) thus recommended taking samples, ideally wedges or cross-sections, closer to the injury in the case of diffuse-porous species so as to increase the potential detection of past events. At our study site, the greater persistence of past injuries on thin-barked broadleaved species and the complexity to detect hidden scars from increment cores probably explain the discrepancies between the scar-counting and dendrogeomorphic approaches.

Interestingly, at the plot scale and in cells A-D, the recurrence intervals computed from the visual inspection of broadleaved stems are comparable to those derived from the analysis of increment cores for conifers (Fig. 8). In the upper part of our plot, characterized by small diameter trees, this similarity allows us to partly rule out the hypothesis formulated by Trappmann and Stoffel (2012) and Favillier et al. (2015) that thick bark constitutes a mechanical barrier that is able to buffer low energy rockfalls and thus damage to the underlying tissues. In other words, we cannot consider at the Saint-Guillaume site that the bark of young conifers is sufficiently thick to protect the underlying cambium from mechanical abrasion caused by rockfall events. Similarly, the scar counting approach does not seem to overestimate rockfall activity by single rocks leaving multiple scars or by rock fragmentation causing a higher number but smaller volume of blocks, leaving multiple impacts (Trappmann and Stoffel 2013; Trappmann et al., 2014).

5.3. Recommendations for hazard zoning

Based on the findings of this study and with the aim of improving cost-benefits ratios in rockfall hazard zoning in mixed forest stands, we recommend future works to:

(1) give priority to the scar-counting approach on small diameter (<15cm) broadleaved stems in the upper part of the slope, i.e. at the vicinity of cliff. Here, trees were demonstrated to yield similar rockfall frequencies to those computed for coniferous trees, but with the much more time-consuming dendrogeomorphic approach;

(2) restrict tree-ring analysis to old conifers, as they are more likely to provide reliable estimates of long recurrence intervals through the identification of tangential rows of traumatic resin ducts. These older conifers are generally located at the lower part of the slope;

(3) exclude, as far as possible, large-diameter broadleaved species from tree-ring analysis due to the remaining complexity of detecting overgrown injuries in tree-ring records. Despite the stringency of our sampling procedure – based on three additional cores taken systematically in the fall line direction at 0.5, 1.0, and 1.5 m – the detection of masked scars indeed represented less than 10% of all GDs found in these trees;

(4) avoid the visual scar counting approach on large-diameter (> 25 cm) conifer trees as their thick bark overgrows rapidly and efficiently past injuries, therefore leading to strong overestimations of recurrence intervals.

6. Conclusions

On forested slopes, the frequency of recent rockfalls can be determined either through (i) the analysis of rockfall injuries remaining visible on the tree surface or (ii) the dating of characteristic growth disturbances (such as growth suppression, tangential rows of traumatic resin ducts or reaction wood) in tree-ring series. In this paper, based on the analysis of 278 broadleaved and conifer trees, we demonstrate that both methods provide similar results on spatial patterns, with an increase of rockfall recurrence intervals down the talus slope and a clear lateral zonation of activity. Paradoxically, and despite the absence of significant differences between recurrence intervals computed between the methods, our results also reveal that rockfall frequency differs quite substantially with tree species and diameter: the visual inspection of conifer stems and the analysis of tree-ring signals in large-diameter broadleaved trees typically leads to an overestimation of recurrence intervals. Based on these results, we recommend to give priority to the scar-counting approach on small diameter broadleaved, frequently impacted stems located in the upper part of the slopes and to restrict the conventional dendrogeomorphic approach to large conifer stems. These recommendations on more suitable practices on how to analyze forest stands in the future according to the tree species and diameter will not only help increase the reliability of recurrence interval maps derived from the analysis of tree growth disturbances, but also improve cost-benefit ratios, thus rendering the approach more attractive for practitioners and natural hazard authorities.

Acknowledgements

This research benefited from the support of the national C2ROP project supported by MEDDE, the French Ministry of Ecology, Sustainable Development and Energy (http://www.c2rop.fr/) and of Labex OSUG@2020 and within the CDP-Trajectories framework, of the French National Research Agency (ANR-15-IDEX-02).

References

Abellán, A., Calvet, J., Vilaplana, J.M., Blanchard, J., 2010. Detection and spatial prediction of rockfalls by means of terrestrial laser scanner monitoring. Geomorphology. 119 (3–4), 162–171. https://doi.org/10.1016/j.geomorph.2010.03.016

Alestalo, J., 1971. Dendrochronological interpretation of geomorphic processes. Fennia. 105, 1–139.

Arbellay, E., Stoffel, M., Bollschweiler, M., Phillips, N., 2010. Wood anatomical analysis of Alnus incana and Betula pendula injured by a debris-flow event, Tree Physiology. 30, Issue 10, 1290–1298, https://doi.org/10.1093/treephys/tpq065

Arbellay, E., Corona, C., Stoffel, M., Fonti, P., Decaulne, A., 2012. Defining an Adequate Sample of Earlywood Vessels for Retrospective Injury Detection in Diffuse-Porous Species. PLoS ONE 7(6). https://doi.org/10.1371/journal.pone.0038824

Baillifard, F., Jaboyedoff, M., Rouiller, J.D., Couture, R., Locat, J., Locat, P., Robichaud, G. and Hamel,. 2004. Towards a GIS-based hazard assessment along the Quebec City Promontory, Quebec, Canada. In: Lacerda, W.A., Ehrlich. M. Fontoura, A.B. and Sayo. A (eds): Landslides Evaluation and stabilization. Balkema, 207–213.

Bannan, M.W., 1936. Vertical resin ducts in the secondary wood of the Abietineae. New Phytol. 35, 11–46.

Bollschweiler, M., Stoffel, M., Schneuwly, D.M., Bourqui, K., 2008. Traumatic resin ducts in Larix decidua stems impacted by debris flows. Tree Physiology. 28, 255–263. DOI : 10.1093/treephys/28.2.255

Bräker, O.U., 2002. Measuring and data processing in tree-ring research – a methodological introduction. Dendrochronologia. 20, 203–216. DOI : 10.1078/1125-7865-00017

Corona, C., Rovera, G., Lopez Saez, J., Stoffel, M., Perfettini, P., 2010. Spatio-temporal reconstruction of snow avalanche activity using tree rings: pierres jean jeanne avalanche talus, Massif de l'Oisans, France. Catena. 83, 107–118. http://dx.doi.org/10.1016/j.catena.2010.08.004

Corona, C., Trappmann, D., Stoffel, M., 2013. Parameterization of rockfall source areas andmagnitudes with ecological recorders: when disturbances in trees serve the calibration and validation of simulation runs. Geomorphology. 202, 33–42.

Corona, C., Lopez Saez, J., Favillier, A., Mainieri, R., Eckert, N., Trappmann, D., Stoffel, M., Bourrier, F., Berger, F., 2017. Modeling rockfall frequency and bounce height from three-dimensional simulation pro-cess models and growth disturbances in submontane broadleaved trees. Geomorphology. 281, 66–77.

Dietze, M., Turowski, J.M., Cook, K.L., Hovius, N., 2017. Spatiotemporal patterns and triggers of seismically detected rockfalls. Earth surface dynamics Discussion, Earth Surf. Dynam. 5, 757–779. https://doi.org/10.5194/esurf-5-757-2017

Dorren, L., 2003. A review of rockfall mechanics and modelling approaches. Progress in Physical Geography: Earth and Environment. 27, 69–87. https://doi.org/10.1191/0309133303pp359ra

Dorren L.K.A., Berger F., le Hir C., Mermin E., Tardif P., 2005. Mechanisms, effects and management implications of rockfall in forests. Forest Ecology and Management. 215, 183–195. DOI : 10.1016/j.foreco.2005.05.012

Dorren L.K.A., Berger F., Putters U.S., 2006. Real-size experiments and 3-D simulation of rockfall on forested and non-forested slopes. Natural Hazards and Earth System Sciences. 6, 145–153. DOI : 10.5194/nhess-6-145-2006

Dorren, L.K.A.., Berger, F., Jonsson, M., Krautblatter, M., Mölk, M., Stoffel, M., Wehrli, A., 2007. State of the art in rockfall–forest interactions. Schweiz. Z. Forstwes. 158:128–141. http://dx.doi.org/10.3188/szf.2007.0128

Dussauge, C., 2003. Statistical analysis of rockfall volume distributions: implications for rockfall dynamics. J. Geophys. Res. 108. http://dx.doi.org/10.1029/2001JB00065

Eichenberger, V., McArdell, B., Christen, M., Trappmann, D. and Stoffel, M., 2017. When tree scars contribute to develop rockfall models. Schweizerische Zeitschrift fur Forstwesen. 168 (2), 84-91. https://doi.org/10.3188/szf.2017.0084

Favillier A., Lopez Saez J., Corona C., Trappmann D., Toe D., Stoffel M., Rovéra G., Berger F., 2015. Potential of two submontane broadleaved species (Acer opalus, Quercus pubescens) to reveal spatiotemporal patterns of rockfall activity. Geomorphology. 246, 35–47. DOI : 10.1016/j.geomorph.2015.06.010

Favillier, A., Mainieri, R., Lopez Saez, J., Berger, F., Stoffel, M., Corona, C., 2017. Dendrogeomorphic assessment of rockfall recurrence intervals at Saint Paul de Varces, Western French Alps. Géomorphologie : relief, processus, environnement [On line],23 - 2.

Favillier, A., Guillet, S., Trappmann, D., Morel, P., Lopez-Saez, J., Eckert, N., Zenhäusern, G., Peiry, J.-L., Stoffel, M., Corona, C., 2018. Spatio-temporal maps of past avalanche events derived from tree-ring analysis: A case study in the Zermatt valley (Valais, Switzerland). Cold Regions Science and Technology. 154, 9–22. https://doi.org/10.1016/j.coldregions.2018.06.004

Fink, S., 1999. Pathological and regenerative plant anatomy. Berlin,Stuttgart: Borntraeger

Franco-Ramos, O., Stoffel, M., Vázquez-Selem, L., 2017. Tree-ring based reconstruction of rockfalls at Cofre de Perote volcano, Mexico. Geomorphology. 290, 142–152. https://doi.org/10.1016/j.geomorph.2017.04.003

Gsteiger P., 1989. Steinschlag, Wald, Relief. Empirische Grundlagen zur Steinschlagmodellierung. Université de Bern, Bern, Suisse (unpublished thesis).

Gsteiger P., 1993. Steinschlagschutzwald. ein beitrag zur abgrenzung, beurteilung und bewirtschaftung. Schweizerische Zeitschrift für Forstwesen. 144, 115–132.

Hungr, O., Evans, S.G., Hazzard, J., 1999. Magnitude and frequency of rockfalls and rockslides along the main transportation corridors of southwestern British Columbia. Canadian Geotechnical Journal. 36, 224–238. DOI : 10.1139/t98-106

Ibsen, ML. and Brunsden, D., 1995. The nature, use and problems of historical archives for the temporal occurrence of landslides, with specific reference to the south coast of Britain Ventnor, Isle of Wight. Geomorphology. 15, 241-258. https://doi.org/10.1016/0169-555x(95)00073-e

Larson, PR., 1994. The vascular cambium. Development and structure. Berlin: Springer.

Lepage, H. and Bégin Y., 1996. Tree-ring Dating of Extreme Water Level Events at Lake Bienville, Subarctic Quebec, Canada, Arctic and Alpine Research. 28:1, 77-84. DOI: 10.1080/00040851.1996.12003150

Migoń, P., Pánek, T., Malik, I, Hrádecký, J., Owczarek, P., Šilhán, K., 2010. Complex landslide terrain in the Kamienne Mountains, Middle Sudetes, SW Poland. Geomorphology. 124(3–4), 200–214. DOI : 10.1016/j.geomorph.2010.09.024

Morel, P., Trappmann, D., Corona, C., Stoffel, M., 2015. Defining sample size and sampling strategy for dendrogeomorphic rockfall reconstructions. Geomorphology. 236, 79–89. DOI : 10.1016/j.geomorph.2015.02.017

Moya J., Corominas J., Pérez Arcas J., Baez, C., 2010. Tree-ring based assessment of rockfall frequency on talus slopes at Solà d'Andorra, Eastern Pyrenees. Geomorphology. 118 (3-4), 393–408. DOI : 10.1016/j.geomorph.2010.02.007

Perret, S., Stoffel, M., Kienholz, H., 2006. Spatial and temporal rockfall activity in a forest stand in the Swiss Prealps – a dendrogeomorphological case study. Geomorphology. 74(1–4), 219–231. https://doi.org/10.1016/j.geomorph.2005.08.009

Rozas, V., 2003. Tree age estimates in Fagus sylvatica and Quercus robur: testing previous and improved methods. Plant Ecol. 167, 193–212. DOI : 10.1023/A:1023969822044

Sachs, T., 1991. Pattern Formation in Plant Tissue. Cambridge University Press, Cambridge.

Sass, O., 2005. Temporal Variability of Rockfall in the Bavarian Alps, Germany, Arctic, Antarctic, and Alpine Research. 37:4, 564-573. DOI: 10.1657/1523-0430(2005)037[0564:TVORIT]2.0.CO;2

Sass O., Oberlechner M. (2012) Is climate change causing increased rockfall frequency in Austria? Natural Hazards and Earth System Sciences. 12, 3209–3216. DOI : 10.5194/nhess-12-3209-2012

Schlappy, R., Jomelli, V., Grancher, D., Stoffel, M., Corona, C., Brunstein, D., Eckert, N., Deschatres, M., 2013. A new tree-ring-based, semi-quantitative approach for the determination of snow avalanche events: use of classification trees for validation. Arct. Antarct. Alp. Res. 45, 383–395. http://dx.doi.org/10.1657/1938-4246-45.3.383

Schneuwly, D.M., Stoffel, M., 2008a. Tree-ring based reconstruction of the seasonal timing, major events and origins of rockfall on a case study slope in the Swiss Alps. Natural Hazards and Earth System Sciences. 8, 203–211. DOI : 10.5194/nhess-8-203-2008

Schneuwly, D.M., Stoffel, M. 2008b. Changes in spatio-temporal patterns of rockfall activity on a forested slope – a case study using dendrogeomorphology. Geomorphology. 102, 522–531. DOI: 10.1016/j.geomorph.2008.05.043

Schneuwly, D.M., Stoffel, M., Bollschweiler, M., 2009a. Formation and spread of callus tissue and tangential rows of resin ducts in Larix decidua and Picea abies following rockfall impacts. Tree Physiology. 29, 281–289. DOI : 10.1093/treephys/tpn026

Schneuwly, D.M., Stoffel, M., Dorren, L.K.A., Berger, F., 2009b. Three-dimensional analysis of the anatomical growth response of European conifers to mechanical disturbance. Tree Physiology. 29, 1247–1257. DOI : 10.1093/treephys/tpp056

Schweingruber, FH., 1996. Tree Rings and Environment Dendroecology. Bern: Paul Haupt.

Selby, M. J., 1993. Hillslope materials and processes (2nd edition), Oxford University Press, New York.

Šilhán, K., Brázdil, R., Pánek, T., Dobrovolný, P., Kašičková, L., Tolasz, R., Turský, O., Václavek, M., 2011. Evaluation of meteorological controls of reconstructed rockfall activity in the Czech Flysch Carpathians. Earth Surface Processes and Landforms. 36, 1898–1909. DOI : 10.1002/esp.2211.

Šilhán, K., Pánek, T and Hradecký, J., 2012. Tree-ring analysis in the reconstruction of slope instabilities associated with earthquakes and precipitation (the Crimean Mountains, Ukraine). Geomorphology. 173–174, 174–184.

Šilhán, K., Pánek, T., Hradecký, J., 2013. Implications of spatial distribution of rockfall reconstructed by dendrogeomorphological methods. Natural Hazards and Earth System Sciences. 13, 1817–1826. DOI : 10.5194/nhess-13-1817-2013

Stoffel, M., 2005. Assessing the vertical distribution and visibility of rockfall scars in trees. Schweizerische Zeitschrift für Forstwesesen. 158, 195–199. DOI : 10.3188/szf.2005.0195

Stoffel, M., Lièvre, I., Monbaron, M., Perret, S., 2005a. Seasonal timing of rockfall activity on a forested slope at Täschgufer (Valais, Swiss Alps) – a dendrochronological approach. Zeitschrit für Geomorphologie. 49, 89–106.

Stoffel, M., Schneuwly, D., Bollschweiler, M., Lièvre, I., Delaloye, R., Myint, M., Monbaron, M., 2005b. Analyzing rockfall activity (1600–2002) in a protection forest - a case study using dendrogeomorphology. Geomorphology. 68, 224 –241.

Stoffel M., Perret S., 2006. Reconstructing past rockfall activity with tree rings: Some methodological considerations. Dendrochronologia. 24, 1–15. DOI : 10.1016/j.dendro.2006.04.001

Stoffel, M., 2006. A review of studies dealing with tree rings and rockfall activity: the role of dendrogeomorphology in natural hazard research. Natural Hazards. 39, 51–70. DOI : 10.1007/s11069-005-2961-z

Stoffel, M., Wehrli, A., Kühne, R., Dorren, L.K.A., Perret, S., Kienholz, H., 2006. Assessing theprotective effect of mountain forests against rockfall using a 3D simulation model.For. Ecol. Manag. 225, 113–122. http://dx.doi.org/10.1016/j.foreco.2005.12.03

Stoffel, M., Bollschweiler, M., 2008. Tree-ring analysis in natural hazards research – an overview. Natural Hazards and Earth System Sciences. 8, 187–202. DOI : 10.5194/nhess-8-187-2008

Stoffel, M., Schneuwly D.M., Bollschweiler M., 2010. Assessing rockfall activity in a mountain forest - implications for hazard assessment. In Stoffel M., Bollschweiler M., Butler D.R., Luckman B.H. (Eds.), Tree Rings and Natural Hazards, Advances in Global Change Research. Springer, Netherlands, 139–155. DOI : 10.1007/978-90-481-8736-2_13

485 Stoffel, M., Bollschweiler, M., Vazquez-Selem, L., Franco-Ramos, O,. Palacios, D., 2011. Dendrogeomorphic dating of rockfalls on lowlatitude,
486 high-elevation slopes: Rodadero, Iztaccıhuatl volcano, Mexico. Earth Surface Processes and Landforms. 36(9), 1209–1217.
487 https://doi.org/10.1002/esp.2146
488 Stoffel, M., Corona, C., 2014. Dendroecological dating of geomorphic disturbance in trees. Tree-Ring Research. 70, 3–20. DOI :
489 10.3959/1536-1098-70.1.3
490 Trappmann, D., Stoffel, M., 2012. Counting scars on tree stems to assess rockfall hazards: A low effort approach, but how reliable?
491 Geomorphology. 180, 180–186. DOI : 10.1016/j.geomorph.2012.10.009
492 Trappmann, D., Stoffel, M., Corona, C., 2014. Achieving a more realistic assessment of rockfall hazards by coupling three-dimensional process
493 models and field-based tree-ring data. Earth Surface Processes and Landforms. 39, 1866–1875. DOI : 10.1002/esp.3580
494 Trappmann, D., Stoffel M., 2015. Visual dating of rockfall scars in Larix decidua trees. Geomorphology. 245, 62–72. DOI :
495 10.1016/j.geomorph.2015.04.030
496 Varnes, D.J., 1978. Slope movement types and processes, in: Landslides: Analysis and Control, edited by: Schuster, R. L. and Krizek, R. J.,
497 Transportation Research Board Special Report 176, National Research Council, Washington, D.C., 11–33.
498 Villalba, R., Veblen, T.T., 1997. Improving estimates of total tree ages based on increment core samples. Ecoscience. 4, 534–542. DOI :
499 10.1080/11956860.1997.11682433
500 Volkwein, A., Scellenberg, K., Labiouse, V., Agliardi, F., Berger, F. Bourrier, F., Dorren, L.K.A., Gerber, W., Jaboyedoff, M., 2011. Rockfall
501 characterisation and structural protection - a review. Nat. Hazards Earth Syst. Sci. 11, 2617 –2651. http://dx.doi.org/10.5194/nhess-11-2617-
502 2011

503 **Captions**

504 **Fig. 1.** The Saint-Guillaume study site (a) is located in the Vercors massif (French Alp), 40km south-west of
505 Grenoble. Rock fragments are detached from several release zones within a roughly 90-m-high, north east-facing
506 cliff (1450-1540 m asl, b). At the study plot (110 × 120m) – delimited by a red polygon (b) – all trees with
507 DBH>5cm were mapped (c) and injuries resulting from past rockfalls inventoried (d, e)

508 **Tab. 1.** Synthesis of rockfall reconstructions based on classical tree-ring analysis and the visual scar counting
509 approach.

510 **Fig. 2.** Spatial distribution and diameters at breast height (DBH; in cm) of trees at the study plot (a) and
511 representative stems that were randomly extracted for the comparison between the visual scar counting and
512 the dendrogeomorphic (tree-ring) approaches (b).

513 **Fig. 3.** Recurrence interval maps derived from the visual scar counting (a) and the dendrogeomorphic
514 approaches (b). Comparison between recurrence intervals derived from both approaches for (c) coniferous and
515 (d) broadleaved trees.

516 **Fig. 4.** Distribution of recurrence interval derived from the visual scar counting approach at the level of cells A-F.

517 **Fig. 5.** Radar chart showing the distributions of the ratio between the numbers of visible / non-visible GD for four
518 stem diameter classes.

519 **Fig.6.** Distribution of recurrence interval derived from the dendrogeomorphic approach at the level of cells A -F.

520 **Tab. 2.** Overview of growth disturbances (GD) identified in tree-ring series. TRD = tangential rows of traumatic
521 resin ducts.

522 **Fig 7.** Distributions of differences between tree age (a), number of growth disturbances (b) and recurrence
523 intervals (c) between the visual scar counting and dendrogeomorphic approaches.

524 **Fig. 8.** Boxplots of recurrence intervals derived from the dendrogeomorphic and visual scar counting approaches
525 at the plot (a) and cell (b-f) scales. Blue and green tone colors are used for broadleaved and conifer trees,
526 respectively.

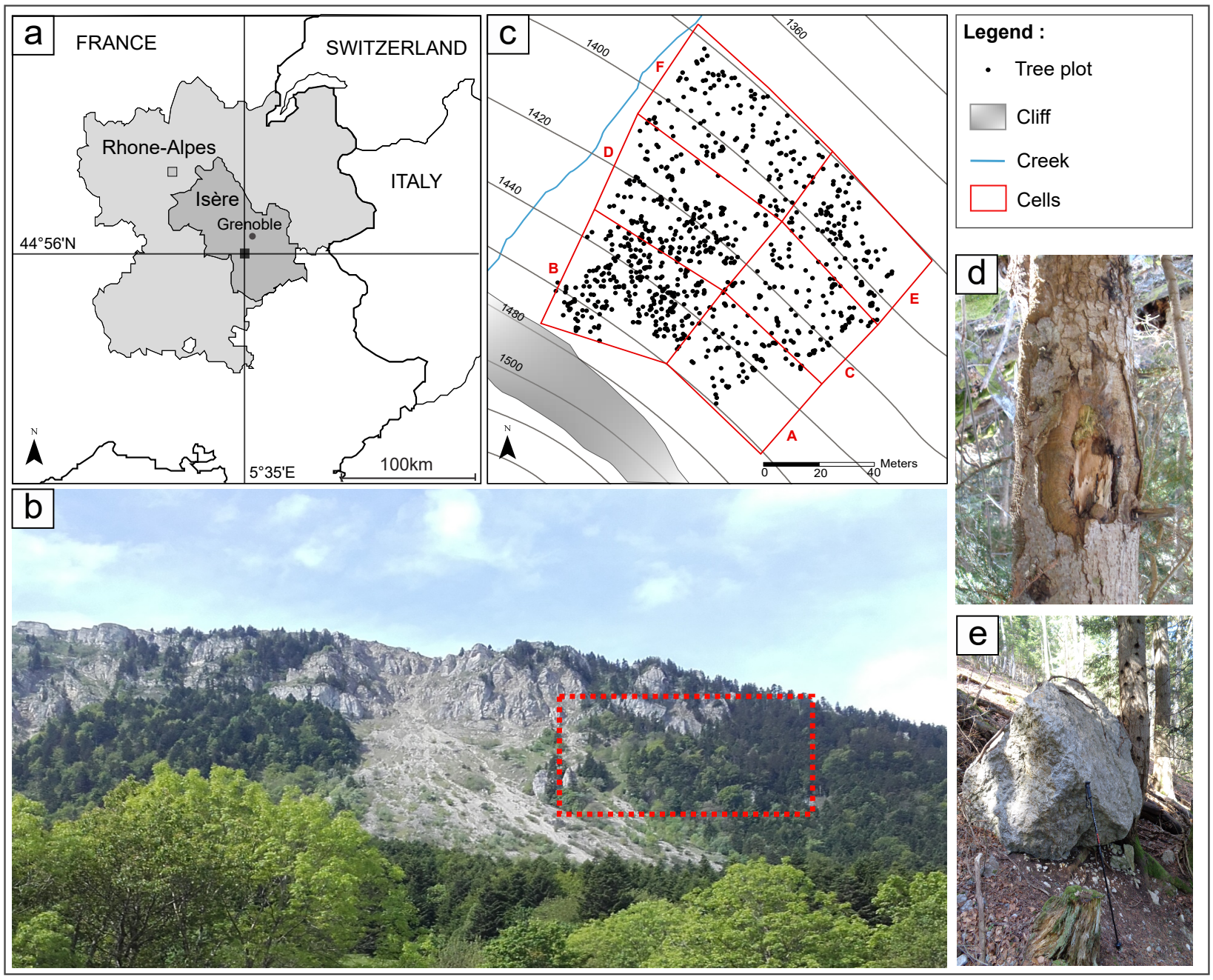
a
FRANCE
SWITZERLAND
ITALY
Rhone-Alpes
Isère
Grenoble
44°56'N
5°35'E
100km
N
c
1400
1420
1440
1480
1500
1360
F
D
B
E
C
A
N
0
20
40
Meters
Legend :
Tree plot
Cliff
Creek
Cells
d
e
b

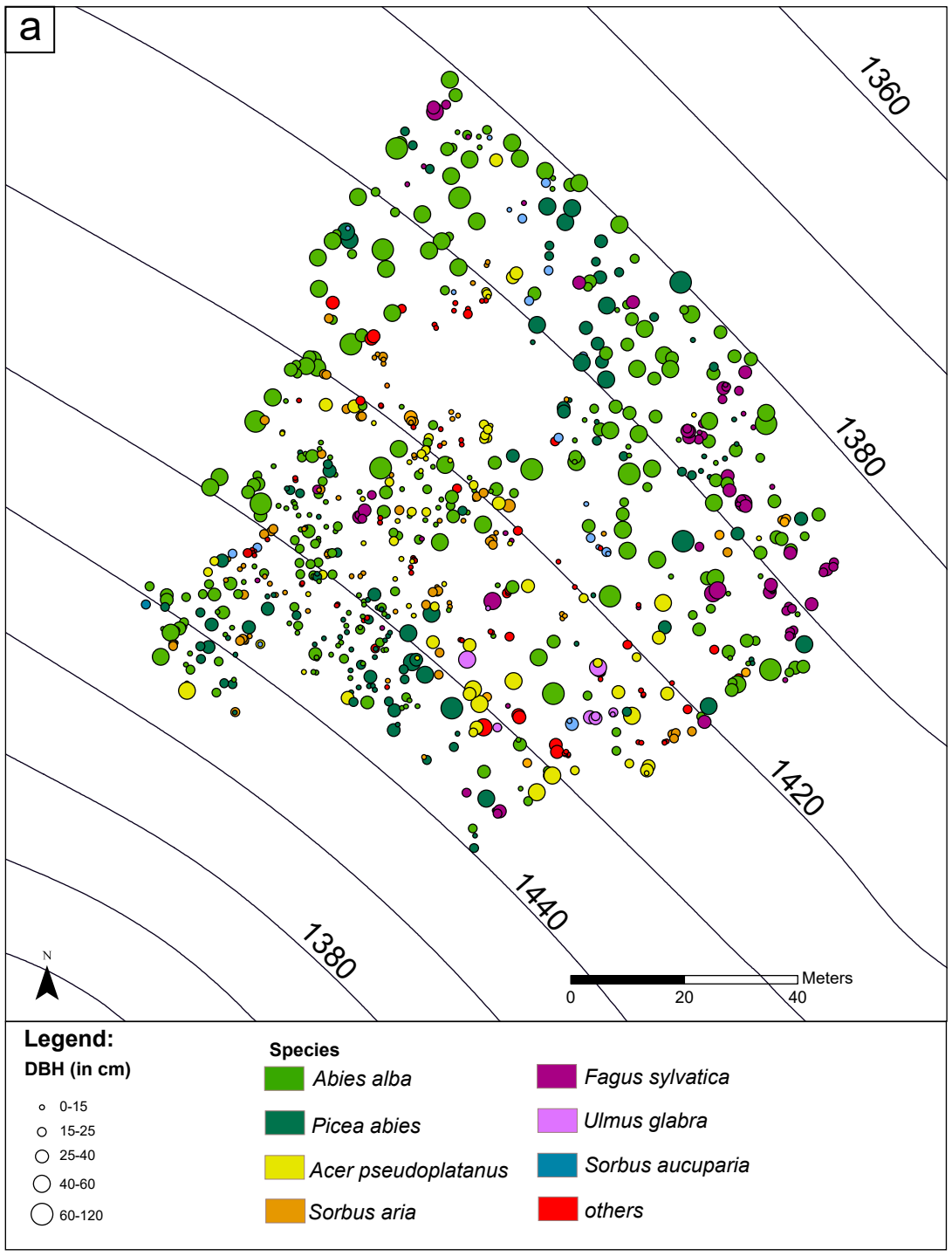
a
1360
1380
1420
1440
1380
N
0
20
40
Meters
Legend:
DBH (in cm)
0-15
15-25
25-40
40-60
60-120
Species
Abies alba
Picea abies
Acer pseudoplatanus
Sorbus aria
Fagus sylvatica
Ulmus glabra
Sorbus aucuparia
others

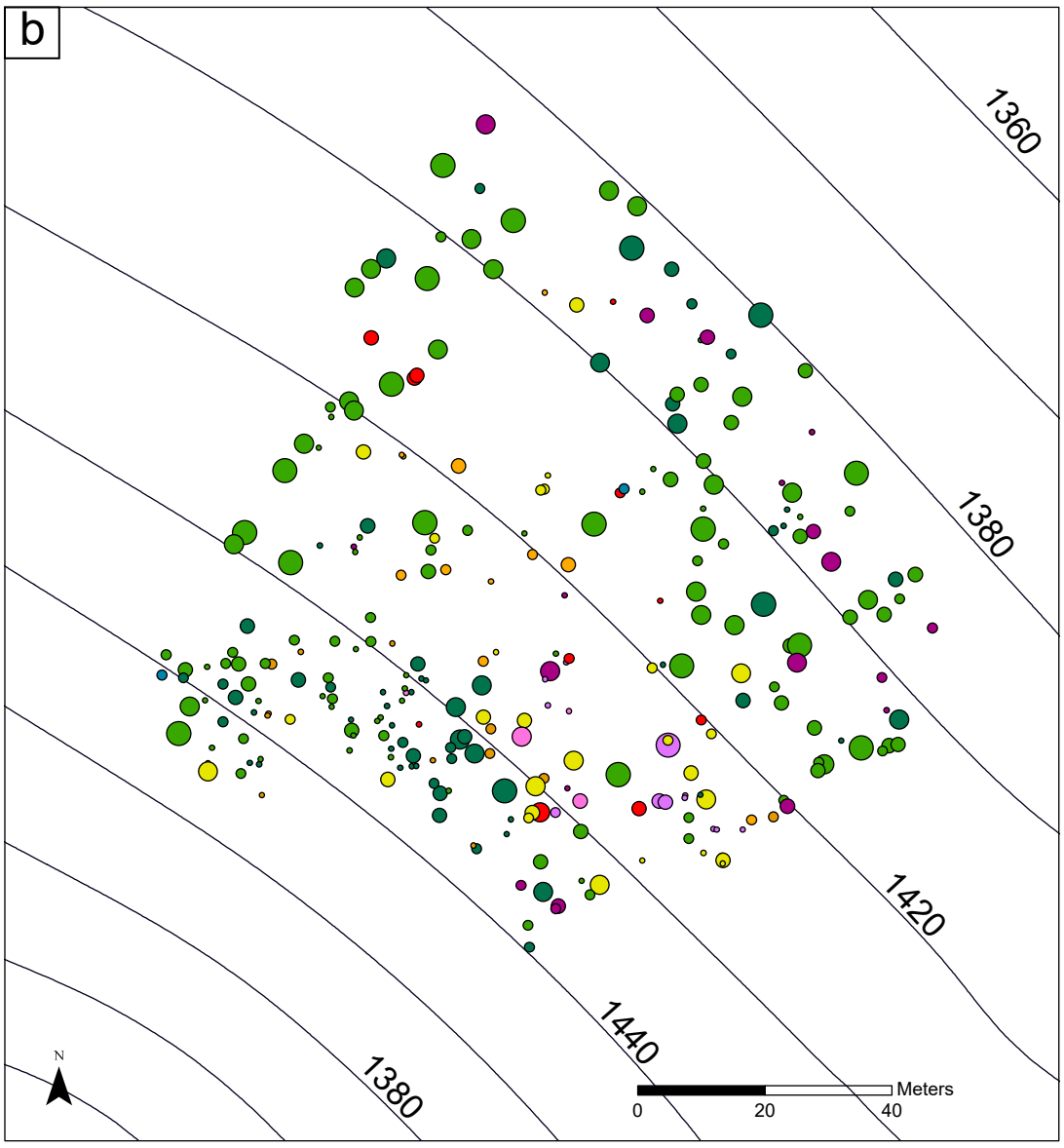
b
1360
1380
1420
1440
1380
N
0
20
40
Meters

(a)

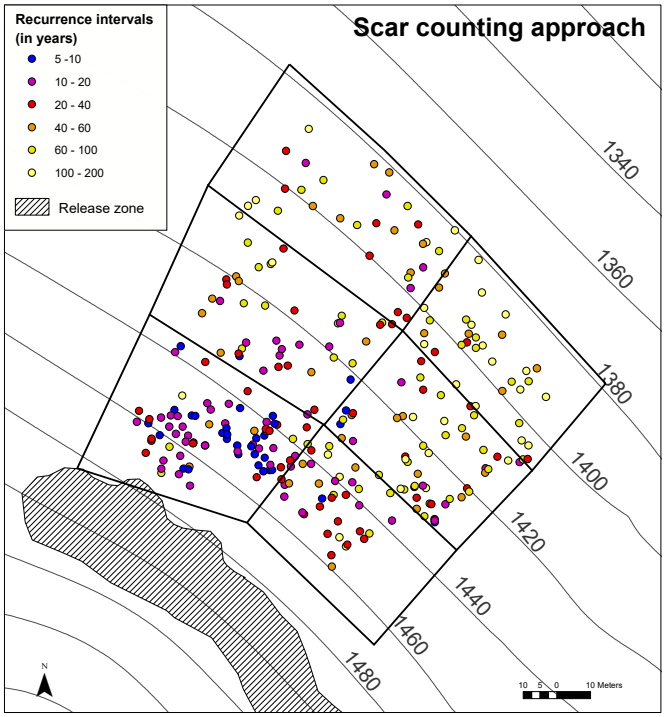
Recurrence intervals (in years)
5 -10
10 - 20
20 - 40
40 - 60
60 - 100
100 - 200
Release zone
Scar counting approach
1340
1360
1380
1400
1420
1440
1460
1480
N
10 5 0 10 Meters

(b)

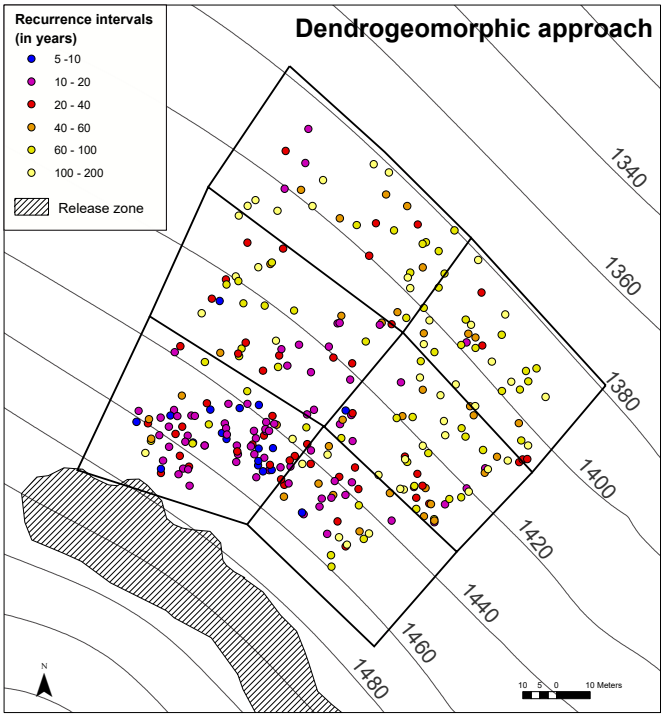
Recurrence intervals (in years)
5 -10
10 - 20
20 - 40
40 - 60
60 - 100
100 - 200
Release zone
Dendrogeomorphic approach
1340
1360
1380
1400
1420
1440
1460
1480
N
10 5 0 10 Meters

(c)

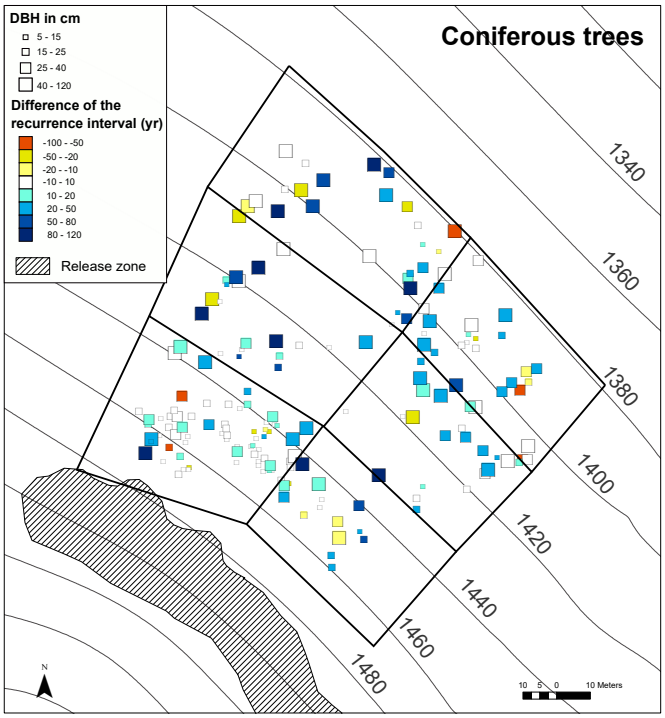
DBH in cm
5 - 15
15 - 25
25 - 40
40 - 120
Difference of the recurrence interval (yr)
-100 - -50
-50 - -20
-20 - -10
-10 - 10
10 - 20
20 - 50
50 - 80
80 - 120
Release zone
Coniferous trees
1340
1360
1380
1400
1420
1440
1460
1480
N
10 5 0 10 Meters

(d)

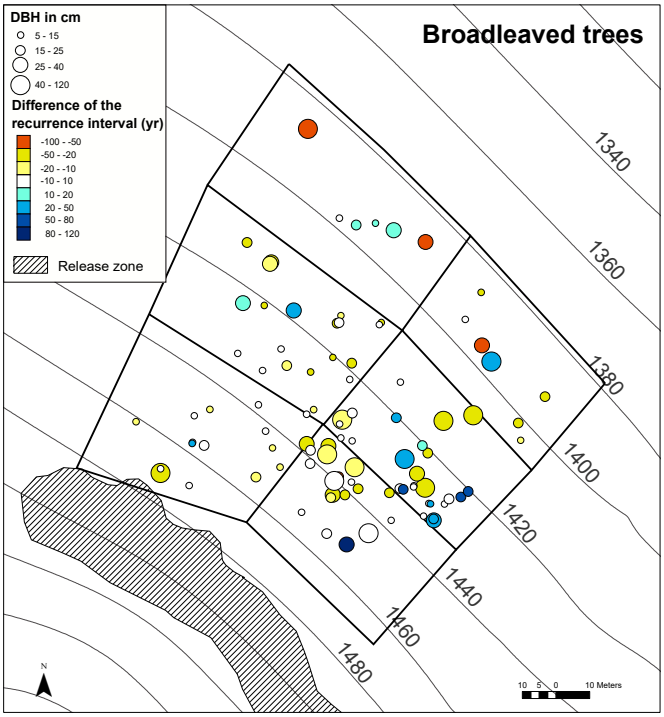
DBH in cm
5 - 15
15 - 25
25 - 40
40 - 120
Difference of the recurrence interval (yr)
-100 - -50
-50 - -20
-20 - -10
-10 - 10
10 - 20
20 - 50
50 - 80
80 - 120
Release zone
Broadleaved trees
1340
1360
1380
1400
1420
1440
1460
1480
N
10 5 0 10 Meters

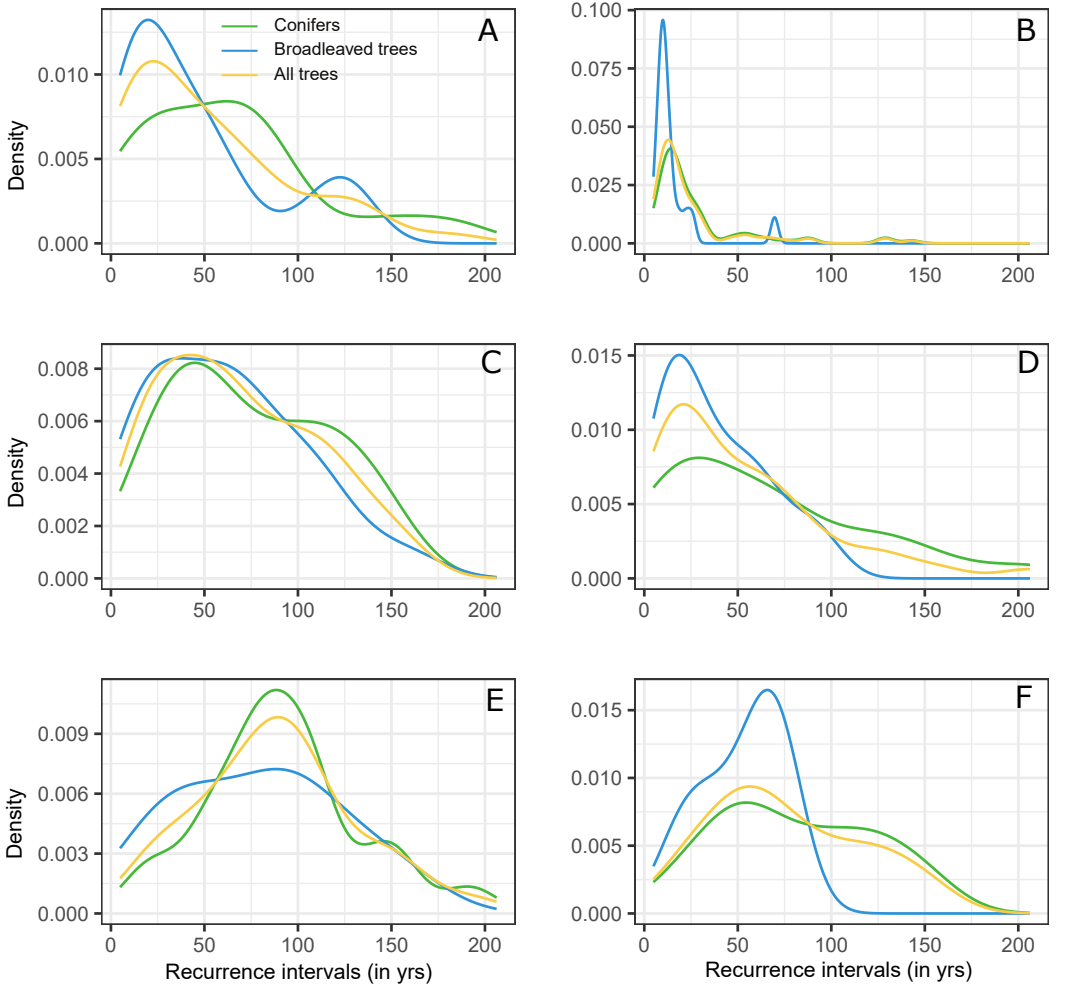
Conifers
Broadleaved trees
All trees
A
B
C
D
E
F
Density
Recurrence intervals (in yrs)

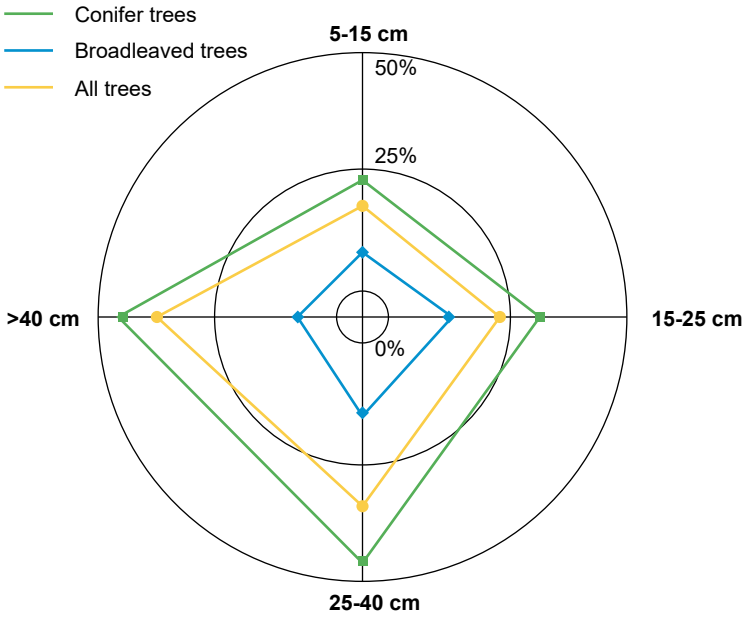
Conifer trees
Broadleaved trees
All trees
5-15 cm
50%
25%
0%
15-25 cm
25-40 cm
>40 cm

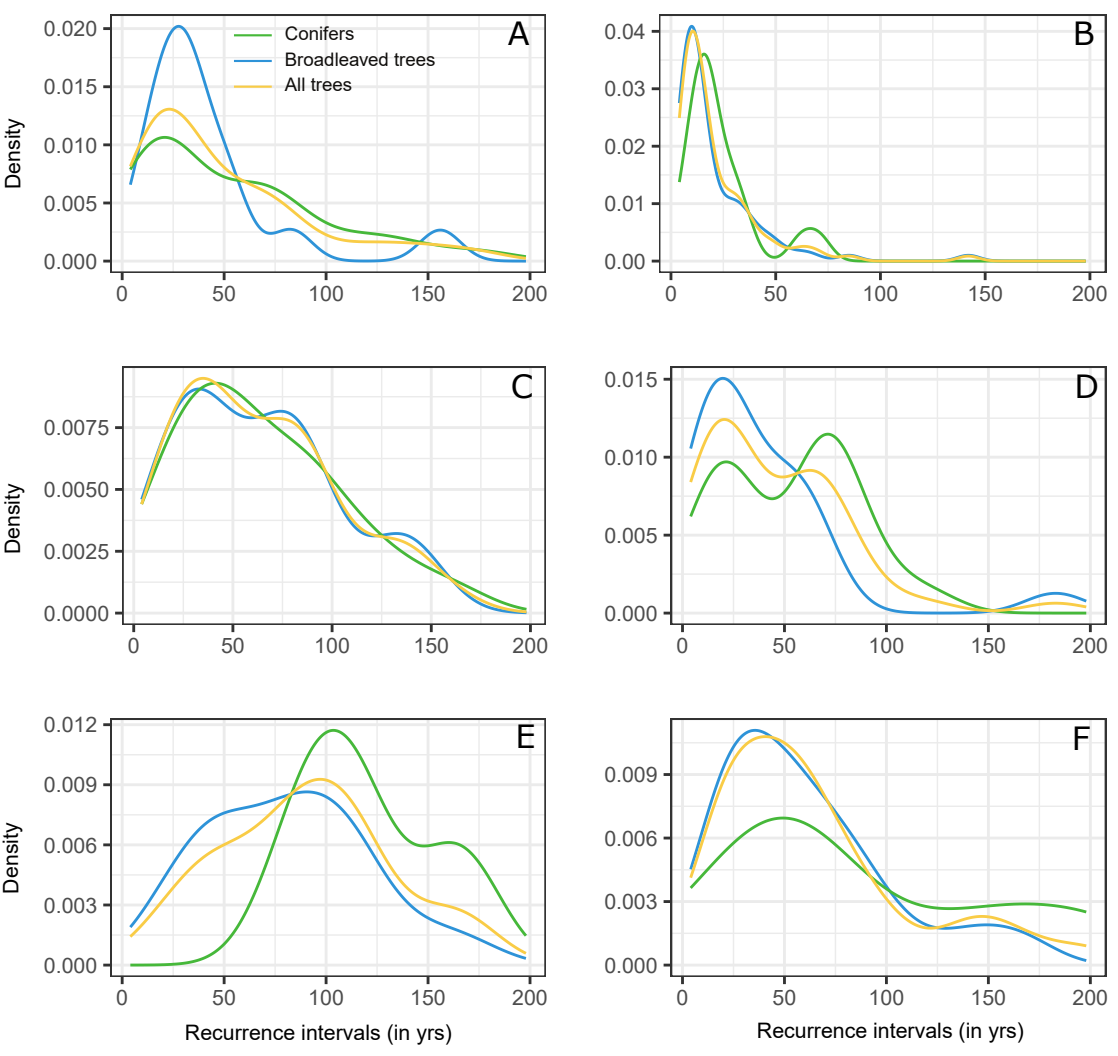
Conifers
Broadleaved trees
All trees
A
B
C
D
E
F
Density
Recurrence intervals (in yrs)

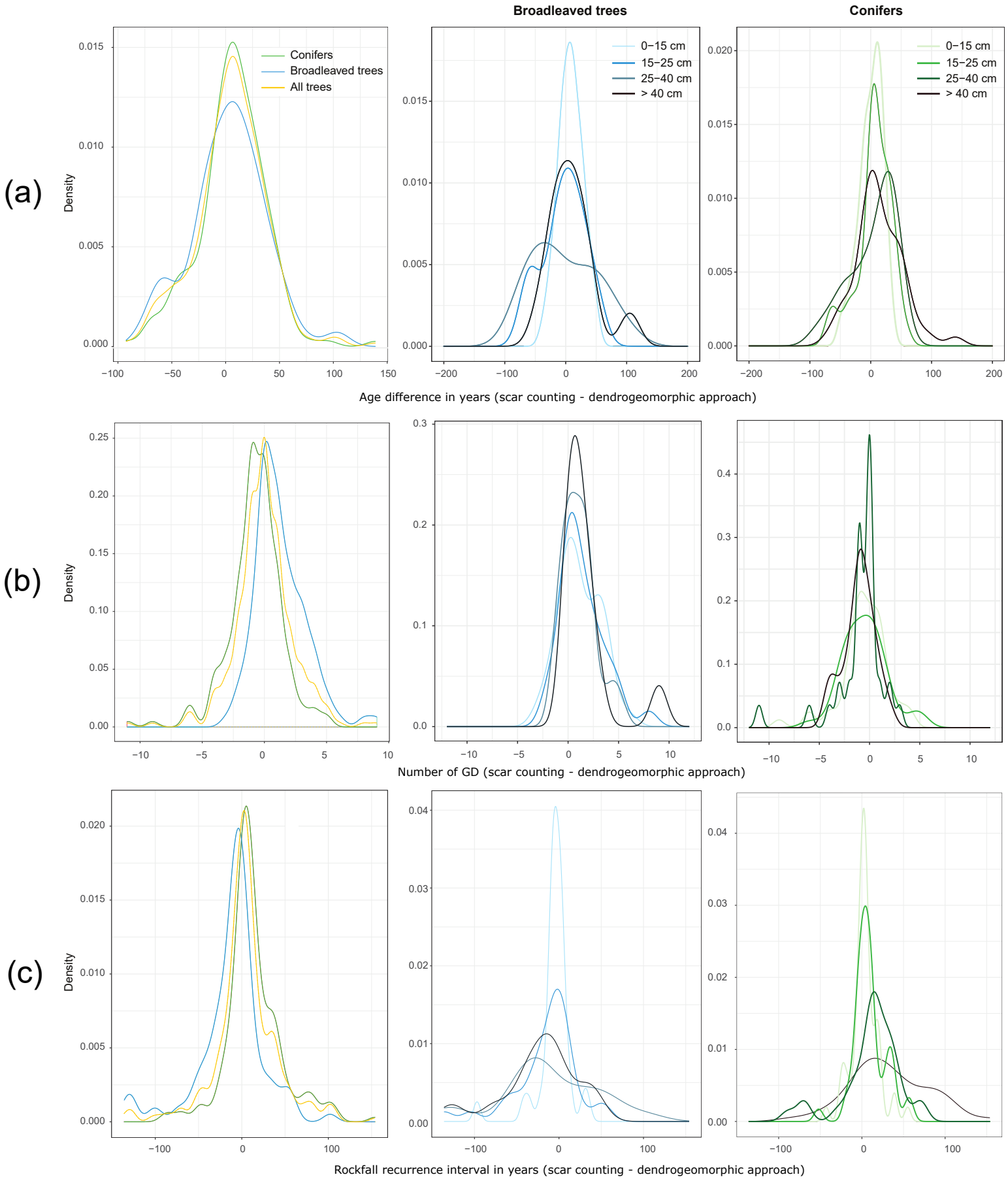
(a)
(b)
(c)
Broadleaved trees
Conifers
Density
Conifers
Broadleaved trees
All trees
0–15 cm
15–25 cm
25–40 cm
> 40 cm
Age difference in years (scar counting - dendrogeomorphic approach)
Number of GD (scar counting - dendrogeomorphic approach)
Rockfall recurrence interval in years (scar counting - dendrogeomorphic approach)

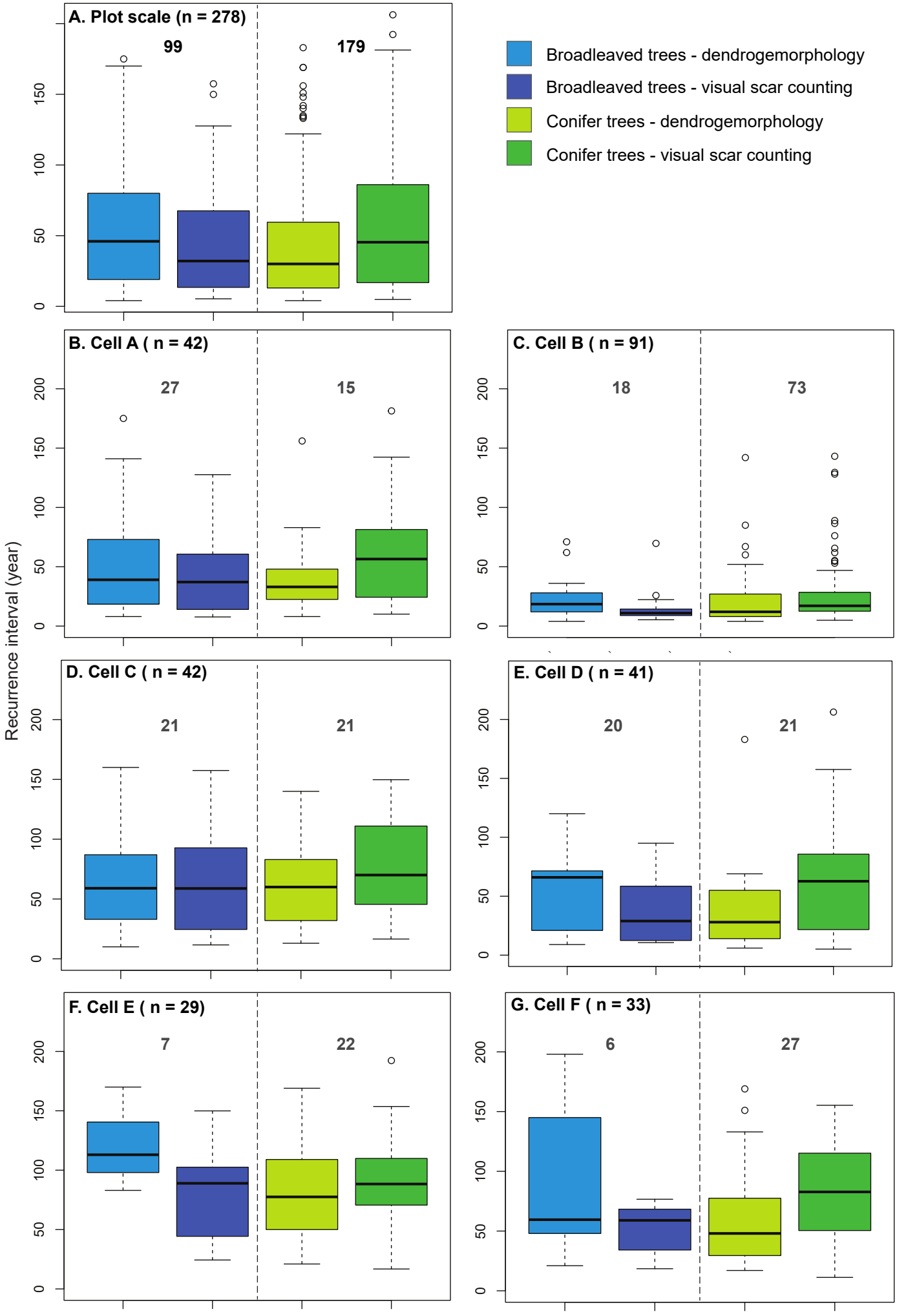
A. Plot scale (n = 278)
99
179
B. Cell A (n = 42)
27
15
C. Cell B (n = 91)
18
73
D. Cell C (n = 42)
21
21
E. Cell D (n = 41)
20
21
F. Cell E (n = 29)
7
22
G. Cell F (n = 33)
6
27
Broadleaved trees - dendrogemorphology
Broadleaved trees - visual scar counting
Conifer trees - dendrogemorphology
Conifer trees - visual scar counting
Recurrence interval (year)
0
50
100
150
200

Authors	Year	Country	Species	Trees sampled	Number of samples	Number of events	Period	Altitude (m)	Sampling strategy	Representation of spatial activity
Gsteiger	1989, 1993	Switzerland	P. abies, F. sylvatica	7	25	56	unknown	\	stem discs	\
Schweingruber	1996	Switzerland	P. abies	30	30	66	1890-1987	\	stem discs	\
Stoffel et al.	2005a	Switzerland	L. decidua	18	270	180	1977-2001	2500	stem discs	\
Stoffel et al.	2005b	Switzerland	L. decidua	135	564	741	1740-2002	1600	increment cores	Recurrence interval
Perret et al.	2006	Switzerland	P. abies	33	33	250	1881-2000	1250	stem discs	Injuries/m²
Schneuwly and Stoffel	2008a	Switzerland	L. decidua, P. abies, Pinus cembra	191	937	745	1957-2006	1600	increment cores, stem discs	Injuries m-1 year-1
Schneuwly and Stoffel	2008b	Switzerland	L. decidua, P. abies, Pinus cembra	32	123	149	1985-2006	1600	stem discs	\
Migoń et al.	2010	Poland	P. abies	32	62	unknown	1877-2007	900	increment cores, stem discs	\
Moya et al.	2010	Andorra	Quercus robur, Quercus ilex	276	375	73	1979-2002	2300	wedges, stem discs	\
Šilhán et al.	2011	Czech Republic	Acer pseudoplatanus, F. sylvatica, P. abies, Sorbus aucuparia, Ulmus glabra	283	1132	989	1931-2008	\	increment cores	\
Stoffel et al.	2011	Mexico	Pinus hartwegii	24	86	63	1924-2008	4300	increment cores, stem discs	Return period
Šilhán et al.	2012	Ukraine	Pinus nigra ssp. Pallasiana	114	456	703	1780-2009	1200	increment cores	\
Trappmann and Stoffel	2013	Austria	P. abies, F. sylvatica	83	194	1417	1819-2009		increment cores, scar count	Return period
Corona et al.	2013	Switzerland	L. decidua, Betula pendula, Corylus avellana L., Fraxinus sp., Sorbus aria (L.) Crantz	133	229	737	1990-2011	1400	increment cores, scar count	Injuries/tree
Trappmann et al.	2014	Switzerland	B. pendula Roth, L. decidua Mill., Populus tremula, P. abies Karst., Fraxinus excelsior, Salix caprea, A. pseudoplatanus, Alnus incana, S. acuparia, Corylus avellana, S. aria Crantz, Prunus avium	1260	202	488	unknown	1400	increment cores, scar count	Frequency
Morel et al.	2015	Switzerland	L. decidua	314	616	372	1908-2014	1800	increment cores, scar count	Frequency
Favillier et al.	2015	France	A. opalus, Q. pubescens	848	0	1230	unknown	600	scar count, forest inventory	Recurrence interval
Trappmann and Stoffel	2015	Switzerland	L. decidua	217	0	217	unknown	1610-2240	scars count	\
Corona et al.	2017	France	A. opalus, Q. pubescens	1004	0	1495	unknown	600	scar count, forest inventory	Injuries/cluster
Franco Ramos et al.	2017	Mexico	Pinus hartwegii	110	212	108	1780-2011	4000	increment cores	Return period
Favillier et al.	2017	France	A. opalus, Q. pubescens	1004	0	1495	unknown	600	scar count, forest inventory	Recurrence interval
Our study	2019	France	A. alba, P. abies, U. glabra, A. pseudoplatanus, S. aria, F. sylvativa	278	1097	810	1801-2017	1350-1490	scar count, forest inventory, increment cores	Recurrence interval

Tab. 1. Synthesis of rockfall reconstructions based on classical tree-ring analysis and the visual scar counting approach.

Growth disturbances	All GD dated		No corresponding damage on stem	
	Number	%	Number	%
Injuries	446	55	92	38
TRD	198	24	76	31
Growth suppression	133	16	63	26
Reaction wood	9	1	5	2
Growth release	24	3	7	3
Total GD	810	100	243	100

Tab. 2. Overview of growth disturbances (GD) identified in tree-ring series. TRD = tangential rows of traumatic resin ducts.